PRAMANA
— journal of
physics

Vol. 70, No. 2
February 2008
pp. 211–220

Localization in disordered systems with interactions

ANGUS MACKINNON
Blackett Laboratory, Imperial College London, South Kensington Campus,
London SW7 2AZ, UK
E-mail: a.mackinnon@imperial.ac.uk

Abstract. We present an improved numerical approach to the study of disorder and interactions in quasi-1D systems which combines aspects of the transfer matrix method and the density matrix renormalization group which have been successfully applied to disorder and interacting problems respectively. The method is applied to spinless fermions in 1D and a generalization to finite cross-sections is outlined.

Keywords. Disorder; interactions; transport; Anderson transition.

PACS Nos 71.30.+h; 71.55.Jv; 72.15.Rn

1. Introduction

It is well-established that in the presence of disorder electron wave functions can become localized. Considerable numerical work has been carried out for non-interacting systems with results reaching a reasonable consensus: theory and experiment are in general qualitative agreement. However, in 3D the calculated value of the universal critical exponent is markedly larger than the experimentally measured value [1]. This seems to suggest that an essential factor is missing from calculations: the obvious candidate is the electron–electron interaction. Furthermore, some have claimed to observe a metal–insulator transition in 2D contrary to the widely accepted scaling theory of Anderson localization [2]. This is often accredited to the effect of interactions. Hence during the last 10 years attention has been switching to this more difficult case. The central problem is that the model becomes a many-body system and so the Hilbert space grows exponentially with system size. This renders an exact numerical calculation far beyond computational capabilities. Nevertheless, several studies have been accomplished, which suggest inclusion of interactions may yield non-trivial behavior.

Shepelyansky [3] performed calculations on two interacting particles. In 1D, interactions caused a large enhancement of localization length. Other work showed that in 2D the effect is possibly stronger leading to delocalization [4].

The most successful method for treating the finite density problem is the density matrix renormalization group (DMRG) approach [5,6]. This works by performing a direct diagonalization but reducing the Hilbert space by systematically discarding

basis states that do not contribute significantly to the ground state. Applying this method to the Anderson interacting model (defined in eq. (1)), a delocalized regime was found for attractive interactions [7,8]. Extensions of DMRG to 2D have encountered problems.

In tackling the problem of localization in a many-body system we encounter several difficulties. The first of these is that most of the conventional measures of localization in a non-interacting system cannot easily be applied to many-body states. The exponential growth of the Hilbert space requires us either to throw away states, in order to keep the problem within manageable dimensions, or to define new quantities which encapsulate all the relevant information while remaining finite.

In developing a suitable algorithm we have to bear in mind that the time required to diagonalize an $N \times N$ matrix scales as N^3. Hence a method which requires the diagonalization of a large number of small matrices is likely to be more efficient than one in which one large matrix is diagonalized.

Recent work on non-interacting systems [1] has demonstrated that the localization must be calculated with an accuracy of at least 0.1% in order for the subsequent finite-size scaling analysis to be reliable. The statistical behavior is such that this implies that a system of length $L_{\max} = 10^6 \lambda_M$ is required, where λ_M is the localization length. We note that this is equivalent to a transmission coefficient $T = 10^{-868,589}$. As this is much less than the machine accuracy, 2×10^{-16}, there is a potential difficulty in fulfilling this condition.

We have developed a new method [9,10] incorporating some of the ideas of DMRG and the transfer matrix method successfully used in the non-interacting case [11,12]. In this paper we will describe an improvement on that method and a generalization to finite cross-section.

2. The method

Before describing the method in detail we consider the conditions which must be fulfilled in order for such a method to be successful.

Our approach is based on a tight-binding model. It can be readily applied to describe any 1D or quasi-1D system, provided interactions are nearest-neighbor. Hence we should not expect the method to describe those phenomena, such as the Coulomb glass [13], which depend on long-range interactions.

2.1 *Hamiltonians*

The approach we describe may be applied to a wide range of different Hamiltonians such as

$$\begin{aligned}\hat{H}_{\text{spinless}} = &\sum_i \varepsilon_i \hat{c}_i^\dagger \hat{c}_i + V \sum_i (\hat{c}_i^\dagger \hat{c}_{i+1} + \hat{c}_{i+1}^\dagger \hat{c}_i) \\ &+ U \sum_i (\hat{c}_i^\dagger \hat{c}_i)(\hat{c}_{i+1}^\dagger \hat{c}_{i+1}) - \mu \sum_i \hat{c}_i^\dagger \hat{c}_i \end{aligned} \tag{1}$$

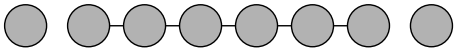

Figure 1. The recursive procedure adds new sites to both ends of a 1D chain at each iteration.

$$\hat{H}_{\text{Hubbard}} = \sum_{i\sigma} \varepsilon_i \hat{c}^\dagger_{i\sigma}\hat{c}_{i\sigma} + V\sum_{i\sigma}(\hat{c}^\dagger_{i\sigma}\hat{c}_{i+1,\sigma} + \hat{c}^\dagger_{i+1,\sigma}\hat{c}_{i\sigma}) + U\sum_i (\hat{c}^\dagger_{i+}\hat{c}_{i+})(\hat{c}^\dagger_{i-}\hat{c}_{i-}) - \mu\sum_{i\sigma}\hat{c}^\dagger_{i\sigma}\hat{c}_{i\sigma} \tag{2}$$

$$\hat{H}_{\text{Bosons}} = \sum_{i} \varepsilon_i \hat{c}^\dagger_{i}\hat{c}_{i} + V\sum_{i}(\hat{c}^\dagger_{i}\hat{c}_{i+1} + \hat{c}^\dagger_{i+1}\hat{c}_{i}) + U\sum_i (\hat{c}^\dagger_{i}\hat{c}_{i})(\hat{c}^\dagger_{i}\hat{c}_{i} - 1) - \mu\sum_{i}\hat{c}^\dagger_{i}\hat{c}_{i} \tag{3}$$

representing spinless fermions (1), the Hubbard model (2) and bosons (3) respectively, where $\hat{c}^\dagger_i$ ($\hat{c}_i$) represent particle creation (annihilation) operators. The first two terms constitute the standard Anderson model [14] used widely in the study of disorder-induced localization. The additional U term represents the interactions while the term in μ, which turns the Hamiltonian into a grand canonical form is required to take account of the changing system size. The value of the parameter μ controls the particle density of the system. $U > 0$ represents normal repulsive interactions whereas $U < 0$ is the attractive case. As with most numerical studies of Anderson localization, zero temperature will be assumed.

2.2 *The recursive method*

In our original approach [9,10] we extended an existing chain by adding an extra site to each end of the system (figure 1).

At each step we obtained a set of states represented as

$$\left\{ \begin{array}{c} \{|0_1\,[L,N]\,0_L\rangle\} \\ \{|1_1\,[L,N-1]\,0_L\rangle\} \\ \{|0_1\,[L,N-1]\,1_L\rangle\} \\ \{|1_1\,[L,N-2]\,1_L\rangle\} \end{array} \right\} \equiv \left[\begin{array}{c} \mathbf{a}_{00} \\ \mathbf{a}_{10} \\ \mathbf{a}_{01} \\ \mathbf{a}_{11} \end{array} \right], \tag{4}$$

where $[L, N]$ represents any state of a system of length, L, containing N electrons. The simplest representation is as a vector made up of four distinct parts, depending on whether the additional sites are occupied or unoccupied. Note that the subvectors $\mathbf{a}_{10}$ and $\mathbf{a}_{01}$ have the same length as they include the same set of states with $N-1$ electrons.

Starting from this representation a density matrix

$$\rho\,(1\ldots0, 0\ldots1) = \mathbf{a}_{10}\cdot\mathbf{a}_{01} \tag{5}$$

may be defined. This may be interpreted as the probability that the addition of an electron on the left results in an electron being omitted from the right. Note that,

due to the indistinguishability of the electrons, we may not demand that the same electron emerges on the right. This quantity may also be related to the dependence on boundary conditions [9,15,16].

It is now possible to define a localization length, λ_M, from

$$\rho(1\ldots0,0\ldots1) \sim \exp(-2L/\lambda_M) \tag{6}$$

$$\Rightarrow \lambda_M = -\lim_{L\to\infty} \frac{2L}{\ln\rho}. \tag{7}$$

2.3 *Reducing the number of basis states*

The purpose of reformulating the basis states and in turn the Hamiltonian in this manner is to enable an approximation to be introduced which keeps the dimension of the Hilbert space roughly constant as sites are added. During each iteration a proportion of the basis states must be thrown away according to some systematic method. This is necessary to keep the calculation to a computationally manageable size. Within the tight-binding framework it is the only approximation in our method.

Initially [9,10] we tried a scheme which fixed a maximum matrix size, chose an appropriate energy cut-off and applied this to the set of states for each particle number. This tended to result in 6–10 groups of retained states for different numbers of particles, those for other particle numbers having ground states above the energy cut-off. Unfortunately this simple criterion failed to result in exponentially decaying behavior of $\rho(1\ldots0,0\ldots1)$, even in the absence of interactions.

Subsequently we realized that fixing an energy cut-off but allowing the number of retained states to fluctuate produced better results and this is the criterion we used in all subsequent work using this model.

3. Results for the single chain model

3.1 *Non-interacting behavior*

The localization properties of a one-dimensional non-interacting chain are well established. For any amount of disorder all eigenstates are localized. The dependence of localization length on disorder is usually quoted as [16]

$$\lambda^{-1} = \frac{W^2}{24(4V^2-\mu^2)}. \tag{8}$$

This is only valid for small disorder. Note that the localization length diverges in the clean limit. Therefore, an important test for the new recursive method is to reproduce this behavior, at least qualitatively.

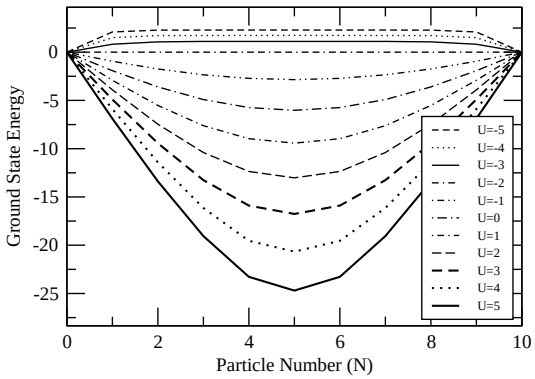

Figure 2. Results from a (clean) short chain of 10 sites demonstrating phase separation for $U < -2$. For each particle number the (grand canonical) ground state energy is plotted. The chemical potential is set to give half-filling as the overall ground state (i.e. $\mu = U$). Plotted energies are grand canonical.

3.2 *Clean phase space*

The second limit to be outlined is the zero disorder phase space. Without randomness the present model can be mapped to a XXZ spin chain model and solved exactly for half-filling [17–20].

At half-filling there are two limiting forms of the ground state with a cross-over regime. For large repulsive interactions a charge density wave (CDW) is observed (i.e. alternate sites are occupied). For attractive interactions and $U > -2$, there is competition between the tendency of the interaction to cause clustering and the kinetic energy which tends to spread the electrons.

For $U < -2$, it is impossible to maintain half-filling within the grand canonical scheme. The ground state is a completely empty or completely full band (i.e. it is unstable to phase separation) as can be seen in figure 2. In fact, as the $U = -2$ limit is reached from above, the ground state energy tends toward being independent of particle number N.

In contrast, for increasing repulsive interactions, above $U = 2$ a charge gap opens up [17,21]. In other words, the CDW above this point corresponds to a Mott insulator state.

3.3 *Typical results*

To illustrate the results obtained with the method described above we show the non-interacting limit in figure 3 and the effect of interactions in figure 4. In neither case are the results wholly satisfactory: the agreement with known results (figure 3) is qualitatively but not quantitatively correct. There is still too much dependence on the number of retained states (figure 4). Although the results appear to be a long way from convergence, the qualitative behavior is as expected.

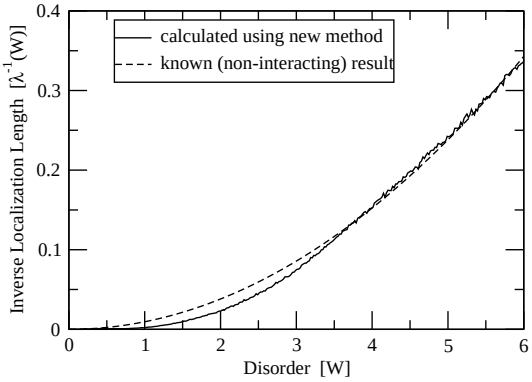

Figure 3. The dependence of inverse localization length on disorder when interactions are turned off. Results from the new method should correspond to known result for the middle of the band. Systems were allowed to extend up to 1000 sites, retaining an average of 480 basis states per iteration. Averages were taken over 1000 disorder realizations.

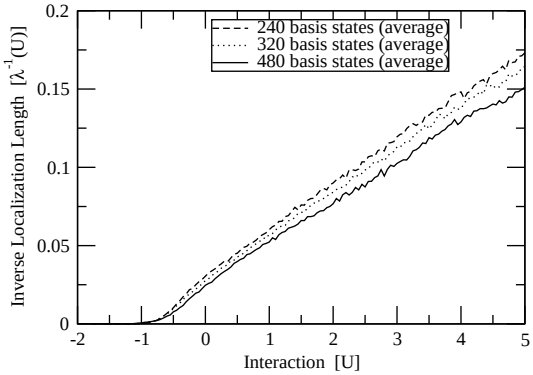

Figure 4. The dependence of localization length on interaction strength. The three lines correspond to different energy cut-off values. Each line is averaged over 1000 systems which are allowed to extend to a maximum of 1000 lattice sites. Disorder $W = 2$.

3.4 *Summary of problems with the original algorithm*

The scalar product in (5) cannot be reliably calculated when it's value drops below the machine accuracy, 2.2×10^{-16}. In practice, this limits the system length to below $L = 1000$. This may be overcome by averaging over smaller systems, but this is only possible when there are no other length scales in the problem which are comparable with or longer than 1000.

At each stage 75% of the states are eliminated. It is not clear whether this constitutes a problem.

The calculation fails for low disorder, $W/V = 2$ ($-\frac{1}{2}W < \varepsilon < +\frac{1}{2}W$), even for $U = 0$: the density matrix does not fall exponentially.

The convergence with the number of retained states is unsatisfactory. It is better when an energy cut-off is used and the number of states is allowed to fluctuate, but convergence is still unacceptable.

4. An improved algorithm

Consider first the density matrix (5) expressed in terms of the site-occupation basis

$$\rho\left(1\ldots0,0\ldots1\right)=\mathrm{Tr}\left[\mathbf{U}^{\dagger}\mathbf{X}_{10}\mathbf{U}\mathbf{X}_{01}\right], \tag{9}$$

where $\mathbf{U}$ is the $(2^L\times K^{(L,N)})$ matrix whose columns are the $K^{(L,N)}$ retained states, $\mathbf{X}_{10}$ is a $(2^L\times 2^L)$ matrix whose elements are all zero except for those which couple two states which differ only that the left-hand end is occupied (left index) or unoccupied (right-index). $\mathbf{X}_{01}$ is the corresponding $(K^{(L,N)}\times K^{(L,N)})$ matrix for the right-hand end.

We now define a new matrix

$$\mathbf{P}^{(L,N)}=\mathbf{U}^{(L,N)\dagger}\mathbf{X}_{10}\mathbf{U}^{(L,N-1)} \tag{10}$$

and note that it obeys a recursion relation

$$\mathbf{P}^{(L+1,N)}=\mathbf{V}^{(L+1,N)\dagger}\begin{bmatrix}\mathbf{P}^{(L,N)} & \mathbf{0}\\ \mathbf{0} & \mathbf{P}^{(L,N-1)}\end{bmatrix}\mathbf{V}^{(L+1,N-1)}, \tag{11}$$

where $\mathbf{V}^{(L+1,N)}$ is the matrix which transforms the eigenvectors for a system of length L into those of length $L+1$

$$\mathbf{U}^{(L+1,N)}=\begin{bmatrix}\mathbf{U}^{(L,N)} & \mathbf{0}\\ \mathbf{0} & \mathbf{U}^{(L,N-1)}\end{bmatrix}\mathbf{V}^{(L+1,N)}. \tag{12}$$

We are now in a position to calculate the required scalar product, and hence the localization length, while only adding a site to one end. This reduces the requirement to throw away states at each iteration to 50%. In fact use of the matrix $\mathbf{P}$ brings an unexpected bonus: due to the product structure of the recursive calculation of $\mathbf{P}$ (11) there is no longer an upper limit on the tractable length of the system. It is possible to calculate $\mathbf{P}$ accurately even when its value falls many orders of magnitude below the machine accuracy. Unexpectedly, other limitations on the algorithm also disappear: the method now behaves sensibly for low disorder and for values of U approaching the limit at $U\to-2$. In fact there are no longer any restrictions on the parameter ranges for which the method behaves sensibly (other than $U<-2$). An additional bonus is that exponential behavior is obtained irrespective of the method used for throwing away states. All these suggest that the earlier results were heavily influenced by the presence of a 2nd length scale which may have been larger than the largest system sizes attainable.

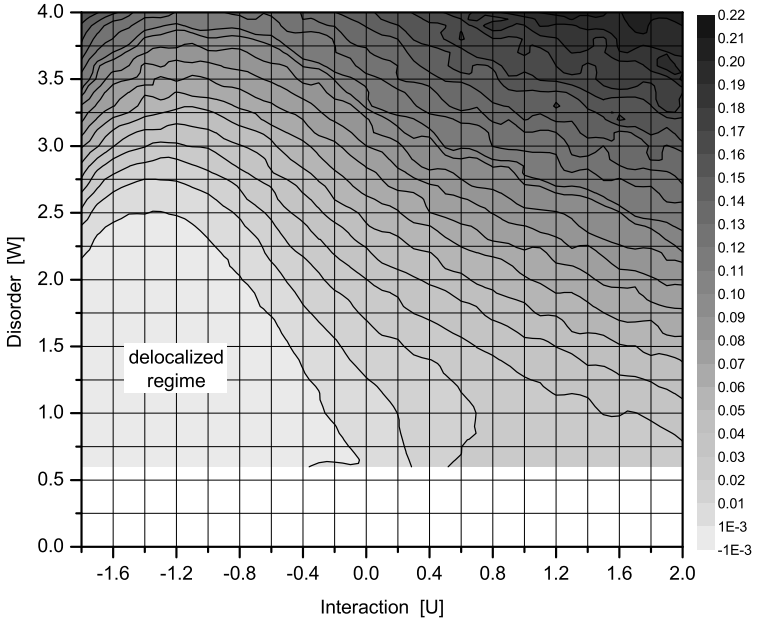

Figure 5. Disorder–interaction phase space plot for the single chain model at half-filling. The contours represent the inverse localization length in intervals of 0.01. The lowest interval corresponds to a localization length greater than 1000 sites. This plot was produced using over 1300 points. Each point was averaged over 250 systems in which chains were allowed to extend to 2000 sites and approximately 240 basis states were retained per iteration. Data for $W < 0.6$ are not shown because the method is unreliable for low disorder.

4.1 *Disorder-interaction phase space*

Figure 5 illustrates the results obtained with the original algorithm and which will be improved by the new method. Note the lack of results for low values of W/V and the fact that the delocalized region appears to come too close to $U = 0$. We are now confident that we are in a position to fill out the gaps in this diagram and to even more reliably map the limits of the extended regime. This is, however, a longer term undertaking.

Nevertheless the results in figure 5 contain many more points than in previous work and refer to significantly larger samples [7,15,21–23]. It should be noted in particular that the limit of the delocalized regime around $W = 2.5$ is a factor of two higher than predicted by Schmitteckert *et al* but lower than in earlier work [21].

5. Generalization to a finite cross-section

Initial attempts to deal with systems of width 2 or the Hubbard model [9] relied on adding a complete set of states for the new site or slice. While this may be

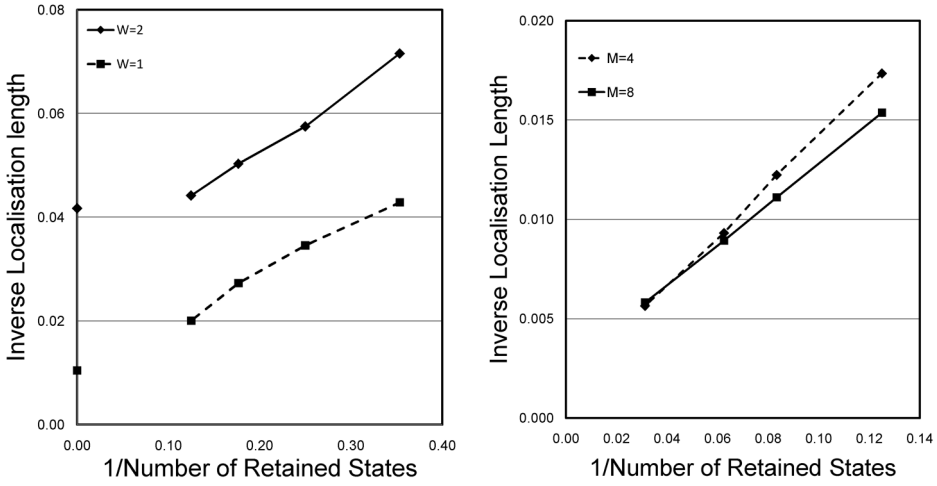

Figure 6. The inverse localization length for $U = 0$ and $W = 1$ and $W = 2$ in 1D (left) and for strips of width $M = 4$ and $M = 8$ (right) plotted against the inverse of the number of retained states. The dots on the left axis (left figure) indicate the known results for the non-interacting system.

made to work for small systems it rapidly becomes prohibitive and, beyond a cross-section $M = 8$, completely intractable. Instead, we consider a method by which additional sites are added to the $L \times M$ system one at a time. In order to do so it is necessary to define a set of new ancillary matrices which are designed to retain the information required to add subsequent atoms to the slice. These are

$$\mathbf{Q}_m^{(L,N)} = \mathbf{U}^{(L,N)\dagger}\mathbf{X}_m^{11}\mathbf{U}^{(L,N)}, \tag{13}$$

$$\mathbf{R}_m^{(L,N)} = \mathbf{U}^{(L,N)\dagger}\mathbf{X}_m^{10}\mathbf{U}^{(L,N)}, \tag{14}$$

where $\mathbf{X}_m^{11}$ is diagonal and unity for all states in which site m is occupied and zero otherwise. $\mathbf{X}_m^{10}$ is similar except that it couples all states which differ only in whether site m is occupied (left-index) or unoccupied (right-index). $\mathbf{Q}$ is required for calculating any interaction terms involving a new site and site m, whereas $\mathbf{R}$ is required for the corresponding hopping terms.

Both $\mathbf{Q}$ and $\mathbf{R}$ may be defined recursively in a similar way to $\mathbf{P}$ and their size is that of the number of retained states.

6. Convergence

While many of the difficulties encountered in our initial attempts to find an algorithm capable of treating the problem of disorder and interactions have been overcome, one major difficulty remains: the convergence of the method with the number of retained states. This is, of course, closely linked to the criterion for eliminating states and it is hoped that it will be possible to improve this in future. As an illustration, consider figures 6. It is quite clear that the examples illustrated are nowhere near convergence.

6.1 *Summary*

We have presented a method for studying disordered and interacting quasi-one-dimensional systems which combines aspects of the transfer matrix and DMRG approaches. While the method works well and is able to study significantly larger systems than have been achieved hitherto, there is still room for improvement. In particular the strategy for reducing the Hilbert space and compensating for the side effects of the reduction is still too simplistic.

References

[1] K Slevin and T Ohtsuki, *Phys. Rev. Lett.* **82(2)**, 382 (1999)
[2] S V Kravchenko, G V Kravchenko, J E Furneaux, V M Pudalov and M d'Iorio, *Phys. Rev.* **B50(11)**, 8039 (1994)
[3] D L Shepelyansky, *Phys. Rev. Lett.* **73(19)**, 2607 (1994)
[4] M Ortuño and E Cuevas, *Europhys. Lett.* **46**, 224 (1999)
[5] S R White, *Phys. Rev. Lett.* **69(19)**, 2863 (1992)
[6] S R White, *Phys. Rev.* **B48**, 10345 (1993)
[7] P Schmitteckert, R A Jalabert, D Weinmann and J-L Pichard, *Phys. Rev. Lett.* **81(11)**, 2308 (1998)
[8] P Schmitteckert, T Schulze, C Schuster, P Schwab and U Eckern, *Phys. Rev. Lett.* **80**, 560 (1998)
[9] J M Carter, *Disorder and interactions in 1D systems*, PhD thesis (University of London, 2003)
[10] J M Carter and A MacKinnon, *Phys. Rev.* **B72**, 024208 (2005)
[11] A MacKinnon and B Kramer, *Phys. Rev. Lett.* **47**, 1546 (1981)
[12] A MacKinnon and B Kramer, *Z. Phys.* **B51**, 1 (1983)
[13] A L Efros and B I Shkloviskii, *J. Phys.* **C8**, L49 (1975)
[14] P W Anderson, *Phys. Rev.* **109(5)**, 1492 (1958)
[15] P Schmitteckert, T Schulze, C Schuster, P Schwab and U Eckern, *Phys. Rev. Lett.* **80(3)**, 560 (1998)
[16] B Kramer and A MacKinnon, *Rep. Prog. Phys.* **56**, 1469 (1993)
[17] H Pang, S Liang and J F Annett, *Phys. Rev. Lett.* **71(26)**, 4377 (1993)
[18] C N Yang and C P Yang, *Phys. Rev.* **150**, 321 (1966)
[19] C N Yang and C P Yang, *Phys. Rev.* **150**, 327 (1966)
[20] C N Yang and C P Yang, *Phys. Rev.* **151**, 258 (1966)
[21] G Bouzerar and D Poilblanc, *J. Phys. I France* **4**, 1699 (1994)
[22] P Schmitteckert and U Eckern, *Phys. Rev.* **B53(23)**, 15397 (1996)
[23] D Weinmann, P Schmitteckert, R A Jalabert and J-L Pichard, *Eur. Phys. J.* **B19**, 139 (2001)